Theoretical Evaluation of Zero Field Splitting Parameters of Mn^{2+} doped $MgNH_4PO_4.6H_2O$ Single Crystal

Ram Kripal, Lal Chandra Shukla

EPR Laboratory, Department of Physics, University of Allahabad, Allahabad, India

Abstract: *Zero field splitting parameters (ZFSPs) D and E of Mn^{2+} doped $MgNH_4PO_4.6H_2O$, magnesium ammonium phosphate hexahydrate (MAP) crystals are evaluated theoretically using crystal field parameters (CFPs) calculated from superposition model. The evaluated theoretical D and E are in reasonable agreement with the experimental values. The experimental conclusion that Mn^{2+} substitutes for Mg^{2+} in MAP is supported by our theoretical study. The D and E values are computed without and with local distortion. The D and E are in reasonable agreement with the experimental values when we take the local distortion into account during calculation.*

Keywords: *A. Inorganic compounds; A. Single crystal; D. Crystal fields; D. Optical properties; D. Electron paramagnetic resonance.*

1. Introduction

Electron paramagnetic resonance (EPR) provides a wealth of information about local site symmetry, magnetic axes and zero field splitting parameters (ZFSPs) of transition metal ions in crystals [1]. Mn^{2+} ion with the ground state ^6S has spin S = 5/2. The electron spins affected by the crystal field via high order interaction become free to orient them in the external magnetic field.

The superposition model (SPM) gives physical and geometrical information existing in crystal field parameters (CFPs) [2, 3]. To apply this model the locations of different ligands in the crystal are necessary and thus the theories of local distortion in crystals are very informative [4].

Theoretical studies of spin Hamiltonian parameters of d^5 ions have been performed by many workers [5, 6]. Various mechanisms contribute to the ground state splitting of the paramagnetic ions in crystals [7] and the study of spin Hamiltonian is generally done by perturbation methods. In majority of the cases, cubic field and the diagonal part of free-ion Hamiltonian are taken as unperturbed terms while the spin-orbit coupling, the low-symmetry field, and the off-diagonal part of free-ion Hamiltonian are assumed as the perturbation terms [8].

The importance of the mineral (or bio-mineral) struvite, $MgNH_4PO_4.6H_2O$ (MAP) is due to its occurrence in human urinary sediments and vesical and renal calculi [9].

MAP has a high degree of recurrence and about 39% of stone suffering patients experience recurrent MAP stones [10]. It is also formed in soils as a reaction product from phosphate fertilizers. It has been the subject of various experimental studies [9]. EPR absorption of Mn^{2+} doped MAP single crystals has been reported earlier [11]. Two possibilities exist for Mn^{2+} site in the MAP crystal, namely, substitutional and interstitial. It is worth to investigate the site of the impurity ion in MAP crystal. It was found [11] that Mn^{2+} ion substitutes at Mg^{2+} site in MAP crystal. In this study, the zero-field splitting parameters (ZFSPs) D and E are evaluated for the Mn^{2+} ion at substitutional Mg^{2+} site in MAP; using CFPs obtained from SPM and perturbation theory [12]. The aim is to get information of Mn^{2+} ion entering the crystal lattice substitutionally or interstitially and also about the distortion taking place in the lattice. The results obtained from this model give reasonable agreement with the experimental values when we consider the local distortion for the Mn^{2+} ion at substitutional Mg^{2+} site in MAP crystal.

This section was provided to the brief introduction of SPM methodology and Hamiltonians. The remaining part of the paper is organized as follows. Section 2 presents the work associated with the CF and ZFS analysis. Section 3 gives the methods employed for calculation of CFPs and ZFSPs. Section 4 provides the results and its discussion based on the analysis performed. In section 5, conclusion of the study and future scope for improvement are given.

2. Crystal Structure

The CF and ZFS analysis have been carried out for various ion-host systems [5, 6, 8, 12]. The crystal structure of $MgNH_4PO_4.6H_2O$ (MAP) crystal is orthorhombic having unit cell parameters a = 0.6941nm, b = 0.6137 nm, c = 1.1199 nm, space group $Pmn2_1$ and Z = 2 [13]. The structure consists of PO_4 tetrahedra, $Mg.6H_2O$ octahedra and NH_4 groups held

together by hydrogen bonding. The PO_4 tetrahedron is regular, with a mean phosphorus-oxygen bond length of 0.1537 nm and the $Mg.6H_2O$ octahedron is very distorted, with a mean magnesium-water oxygen bond length of 0.2071 nm. The mean water oxygen hydrogen bond length is found to be 0.0778 nm. The orientations of the *(x, y, z)* axes (SAAS-symmetry adopted axis system) relative to the *(a, b, c)* crystallographic axes in the crystal are *(x → c, y → a, z → b)* as shown in Fig. 1.

3. Theoretical Investigation

The resonance magnetic fields are analyzed using the spin Hamiltonian [14, 15],

$$\mathcal{H} =$$

$$\mu_B BgS + D\left\{S_z^2 - \frac{1}{3}S(S+1)\right\} + E(S_x^2 - S_y^2) + \frac{a}{6}[S_x^4 + S_y^4 + S_z^4 - \frac{1}{5}S(S+1)(3S^2 + 3S+1)]$$

$$(1)$$

where g is the spectroscopic splitting factor, μ_B is the Bohr magneton and B is the external magnetic field. D and E are the second rank axial and rhombic ZFSPs, while *a* is the fourth rank cubic ZFSP [16, 17]. The maximum overall splitting of the EPR spectrum is taken along the z axis and the minimum along the x axis [18]. The laboratory axes (x, y, z) are parallel to the crystallographic axes. The local site symmetry axes, i. e. the symmetry adopted axes (SAA) are the nearly orthogonal directions of metal-ligand bonds. The Z-axis of symmetry adopted axis system (SAAS) in two equivalent sites is coincident with the crystal **b**-axis and the other two axes (X, Y) lie in the ac plane (Fig. 1). This indicates that Mn^{2+} substitutes Mg^{2+} in the crystal lattice. The ionic radius of Mn^{2+} ion 080 nm [19] is slightly larger than the ionic radius of Mg^{2+} (0.066 nm), thus Mn^{2+} ion can substitute at the site of Mg^{2+} with some distortion.

The ZFSPs of Mn^{2+} ions at two equivalent sites are determined using the perturbation theory [20, 21]. These values are then compared with the experimental ones.

The spin Hamiltonian of a d^5 (^6S state) ion is written as sum of free ion ($\mathcal{H}_o$), spin-orbit coupling ($\mathcal{H}_{so}$), spin-spin coupling ($\mathcal{H}_{ss}$) and crystal field ($\mathcal{H}_c$) Hamiltonians,

$$\mathcal{H} = \mathcal{H}_o + \mathcal{H}_{so} + \mathcal{H}_{ss} + \mathcal{H}_c \qquad (2)$$

with

$$\mathcal{H}_c = \sum B_{kq} C_q^{(k)} \qquad (3)$$

where B_{kq} are the crystal-field parameters and $C_q^{(k)}$ are the Wybourne spherical tensor operators. For the crystal field of orthorhombic symmetry, $B_{kq} \neq 0$ only with k = 2, 4, q = 0, 2, 4. The crystal-field theory has been widely used for the study of spin Hamiltonian parameters of transition ions in different crystals [12, 22-24]. In this study, the CFPs, B_{kq} are calculated using SPM [20].

In MAP crystal the local symmetry around Mn^{2+} ions is taken to be orthorhombic of type I (OR-I) [11, 19]. In OR-I symmetry, the ZFSPs D and E are given by [12]

$$D = \left(\frac{3\varsigma^2}{70P^2D}\right)[-B_{20}^2 - 21\varsigma B_{20} + 2B_{22}^2] + \left(\frac{\varsigma^2}{63P^2G}\right)[-5B_{40}^2 - 4B_{42}^2 + 14B_{44}^2]$$

$$E = \left(\frac{\sqrt{6}\varsigma^2}{70P^2D}\right)[2B_{20} - 21\varsigma]B_{22} + \left(\frac{\varsigma^2}{63P^2G}\right)[3\sqrt{10}B_{40} + 2\sqrt{7}B_{44}]B_{42}$$

$$(4) \text{ and } (5)$$

where P = 7B+7C, G = 10B+5C, D = 17B+5C. B and C are Racah parameters, giving electron-electron repulsion and ς is the spin-orbit coupling parameter. It is found that the values of B and C for transition metal ion in a crystal are less than those of the free ion. By taking the average covalency parameter N, we can write the Racah parameters [20, 25] and spin-orbit coupling parameter as: B = N^4B_0, C = N^4C_0, ς = $N^2 \varsigma_0$, where B_0 and C_0 are Racah parameters for free ion and ς_0 is free ion spin-orbit coupling parameter. For free Mn^{2+}ion, B_0 = 960 cm^{-1}, C_0 = 3325 cm^{-1} and ς_0 = 336 cm^{-1} are used [20].

Taking the values of Racah parameters (B = 917 cm^{-1}, C = 2254 cm^{-1}) evaluated from optical study of the Mn^{2+} ion with O ligands [26], the average parameter N is obtained from N = ($\sqrt{B/B_0} + \sqrt{C/C_0}$)/2.

The CFPs from SPM are given [12, 27] by

$$B_{kq} = \sum_j \overline{A_k}(R_j)K_{kq}(\theta_j, \phi_j) \qquad (6)$$

where the co-ordination factor $K_{kq}(\theta_j, \varphi_j)$ is an explicit function of the angular position of the ligand. The intrinsic parameter $\overline{A_\kappa}(R_j)$ is represented as

$$\overline{A_k}(R_j) = \overline{A_k}(R_0)\left(\frac{R_0}{R_j}\right)^{t_k}$$

where R_j is the distance between the d^n ion and the ligand, $\overline{A_k}(R_0)$ represents the intrinsic parameter of the reference crystal, t_k is the power law exponent and R_0 is the reference distance between the metal and ligand. For Mn^{2+} doped in different crystals having various ligands, $t_2 = 3$ and $t_4 = 5$ [24]. The above values in this calculation gave non-standard E/D ratio. Therefore we have used $t_2 = 3$ and $t_4 = 4$ in our calculation to get standard ratio E/D (<0.33) [18]. As the co-ordination around Mn^{2+} ion is octahedral, $\overline{A_4}$ and Dq have relation given by [28]

$$\overline{A_4}(R_0) = \frac{3}{4}Dq$$

From optical study [26], the value of Dq = 756 cm^{-1}. Thus, the relation gives the value of $\overline{A_4}(R_0)$ = 567 cm^{-1}. It is noted that for $3d^5$ ions the ratio of $\overline{A_2}(R_0)$ and $\overline{A_4}(R_0)$ lies between 8 to 12 [20, 29, 30]. In this study, $\dfrac{\overline{A_2}}{\overline{A_4}}$ =10 is taken, which gives $\overline{A_2}$ = 5670 cm^{-1}.

4. Results and Discussion

The CFPs B_{kq} of Mn^{2+} ion at two equivalent sites are calculated using SPM, parameters $\overline{A_2}$ and $\overline{A_4}$ and arrangement of ligand ions around Mn^{2+} ion (Fig. 1). Atomic coordinates in MAP crystal and bond length R (without and with distortion) along with angle θ, φ (one site) are shown in Table 1. The calculated CFPs and ZFSPs along with reference distance R_0 are shown in Table 2. It is noted from Table 2 that the value of R_0 = 0.104 nm smaller than the lowest of four ligand distances from the central metal ion (0.2046 nm) together with local distortion provide ZFSPs for all the equivalent sites in reasonable agreement with the experimental values [11]. The S2 transformation has been used to get standard ratio of E/D [18]. The ZFSPs calculated using R_0 = 0.104 nm and without local distortion are slightly larger than the experimental values. For comparison the interstitial sites for Mn^{2+} ions are also calculated. The calculated values of ZFSPs are quite different from the experimental ones and hence are not given here.

Using CFPs and CFA program [31, 32] with OR-I symmetry of the crystal field the optical spectra of Mn^{2+} doped MAP crystals are calculated. The energy levels of the impurity ion are determined by diagonalization of the complete Hamiltonian within the $3d^N$ basis of states in the intermediate crystal field coupling scheme. The calculated energy values are shown in Table 3 together with the experimental values for comparison. There is a reasonable agreement between the two. Thus, the results obtained using superposition model support the experimental result that Mn^{2+} ions substitute at Mg^{2+} site in the crystal [11].

5. Conclusions

CFPs and ZFSPs for Mn^{2+} ion doped MAP have been determined using superposition model and perturbation theory, respectively. The obtained ZFSPs show a reasonable agreement with the experimental values. The calculated optical spectra are also in reasonable agreement with the experimental one. The inference on the basis of superposition model supports the experimental result that Mn^{2+} ions substitute at Mg^{2+} site in the MAP crystal. Modeling methods employed in this study may be useful in future to correlate EPR and optical data for various ion-host systems. The combined modeling approaches: CF, ZFS and Microscopic Spin Hamiltonian can provide better correlation of EPR and optical data.

References

[1] J. A. Weil, J. R. Bolton, Electron Paramagnetic Resonance: Elementary Theory and Practical Applications, 2nd ed., Wiley, New York, 2007.

[2] M. I. Bradbury, D. J. Newman, Ratios of crystal field parameters in rare earth salts, Chem. Phys. Lett. **1** (1967) 44-45.

[3] D. J. Newman, On the g-shift of S-state ions, J. Phys. C: Solid State Phys. **10** (1977) L315-L318.

[4] E. Siegel and K. A. M$\ddot{u}$ller, Local position of Fe^{3+} in ferroelectric $BaTiO_3$, Phys. Rev. B **20** (1979)3587-95.

[5] Y. Y. Yeung, Local distortion and zero-field splittings of $3d^5$ ions in oxide crystals, J. Phys. C: Solid State Phys. **21**(1988)2453-61.

[6] W. L. Yu, Cubic zero-field splitting of a [6]S state ion, Phys. Rev. **B 39** (1989) 622-632.

[7] M. G. Brik, C. N. Avram, N. M Avram, Calculations of spin Hamiltonian parameters and analysis of trigonal distortions in $LiSr(Al,Ga)F_6:Cr^{3+}$ crystals, Physica **B 384** (2006) 78-81.

[8] Z. Y. Yang, An investigation of the EPR zero-field splitting of Cr^{3+} ions at the tetragonal site and the Cd^{2+} vacancy in $RbCdF_3:Cr^{3+}$ crystals, J. Phys.: Condens. Matter **12** (2000) 4091-4096.

[9] F. Abbona, R. Boistelle, Growth morphology and crystal habit of struvite crystals ($MgNH_4PO_4 \cdot 6 H_2O$), J. Cryst. Growth 46 (1979) 339-354; and Refs therein.

[10] E. Takasaki, An Observation on the Composition and Recurrence of Urinary Calculi, Urol. Intern. 30 (1975) 228-236.

[11] P. Chand, O. P. Agarwal, Electron paramagnetic resonance study of doped synthetic crystals of struvite and its zinc analogue, Spectrochim. Acta A47 (1991)775-783.

[12] W. L. Yu, M.G. Zhao, Spin-Hamiltonian parameters of [6]S state ions, Phys. Rev. B **7** (1988) 9254-9267.

[13] A. Whitaker, J. W. Jeffery, The Crystal Structure of Struvite, $MgNH_4PO_4.6H_2O$, Acta Cryst. B26(1970)1429-1440.

[14] A. Abragam, B. Bleaney, Electron Paramagnetic Resonance of Transition Ions, Clarendon Press, Oxford, 1970.

[15] C. Rudowicz, Concept of spin Hamiltonian, forms of zero field splitting and electronic Zeeman Hamiltonians and relations between parameters used in EPR. A critical review, Magn. Reson. Rev. 13 (1987) 1-89.

[16] C. Rudowicz, H. W. F. Sung, Can the electron magnetic resonance (EMR) techniques measure the crystal (ligand) field parameters?, Physica B 300 (2001) 1-26.

[17] C. J. Radnell, J. R. Pilbrow, S. Subramanian, M. T. Rogers, Electron paramagnetic resonance of Fe^{3+} ions in $(NH_4)_2SbF_5$, J. Chem. Phys. 62 (1975) 4948-4952.

[18] C. Rudowicz, R. Bramley, On standardization of the spin Hamiltonian and the ligand field Hamiltonian for orthorhombic symmetry, J. Chem. Phys. 83 (1985) 5192-5197.

[19] B. N. Figgis, M. A. Hitchman, Ligand Field Theory and its Applications, Wiley, New York, 2000.

[20] T. H. Yeom, S. H. Choh, M. L. Du and M. S. Jang, EPR study of Fe3+ impurities in crystalline $BiVO_4$, Phys. Rev. B 53 (1996) 3415- 3421.

[21] C. Rudowicz, S. K. Misra, SPIN-HAMILTONIAN FORMALISMS IN ELECTRON MAGNETIC RESONANCE (EMR) AND RELATED SPECTROSCOPIES, Appl. Spectrosc. Rev. 36 (2001) 11–63.

[22] Z. Y. Yang, C. Rudowicz, Y. Y. Yeung, Microscopic spin-Hamiltonian parameters and crystal field energy levels for the low C_3 symmetry Ni^{2+} centre in $LiNbO_3$ crystals, Physica B 348 (2004) 151–159.

[23] Z. Y. Yang, Y. Hao, C. Rudowicz, Y. Y. Yeung, Theoretical investigations of the microscopic spin Hamiltonian parameters including the spin–spin and spin–other-orbit interactions for $Ni^{2+}(3d^8)$ ions in trigonal crystal fields, J. Phys.: Condens. Matter 16 (2004) 3481–3494.

[24] T. H. Yeom, Y. M. Chang, S. H. Choh, C. Rudowicz, Experimental and Theoretical Investigation of Spin-Hamiltonian Parameters for the Low Symmetry Fe^{3+} Centre in $LiNbO_3$, Phys. Stat. Sol. b185 (1994) 409–415; C. Rudowicz, Z. Y. Yang, Y. W. Lun, Crystal field analysis for $3d^4$ and $3d^6$ ions with an orbital singlet ground state at orthorhombic and tetragonal symmetry sites, J. Phys. Chem. Solids, 53 (1992) 1227-1236.

[25] C. K. Jorgensen, Modern Aspects of Ligand Field Theory, North- Holland, Amsterdam, 1971, p.305.

[26] R. Kripal, H. Govind, S. K. Gupta, M. Arora, EPR and optical absorption study of Mn2+-doped zinc ammonium phosphate hexahydrate single crystals, Physica B, 392 (2007) 92-98.

[27] D. J. Newman, B. Ng, The superposition model of crystal fields, Rep. Prog. Phys. 52(1989)699-763.

[28] D. J. Newman, B. Ng (Eds.), Crystal Field Handbook, Cambridge University Press, Cambridge, 2000.

[29] D. J. Newman, D. C. Pryce, W. A. Runciman, Superposition model analysis of the near infrared spectrum of Fe (super 2+) in pyrope-almandine garnets, Am. Miner. 63 (1978) 1278-1281.

[30] A. Edgar, Electron paramagnetic resonance studies of divalent cobalt ions in some chloride salts, J. Phys. C: Solid State Phys. 9 (1976) 4303-4314.

[31] P. Gnutek, Z. Y. Yang and C. Rudowicz, Modeling local structure using crystal field and spin Hamiltonian parameters: the tetragonal $Fe_K^{3+}–O_I^{2-}$ defect center in $KTaO_3$ crystal, J. Phys.: Condens. Matter 21, 455402 (2009)(11pp).

[32] Y. Y. Yeung, C.Rudowicz, Crystal Field Energy Levels and State Vectors for the $3d^N$ Ions at Orthorhombic or Higher Symmetry Sites, Issue 1, J. Comput. Phys. 109 (1993) 150-152.
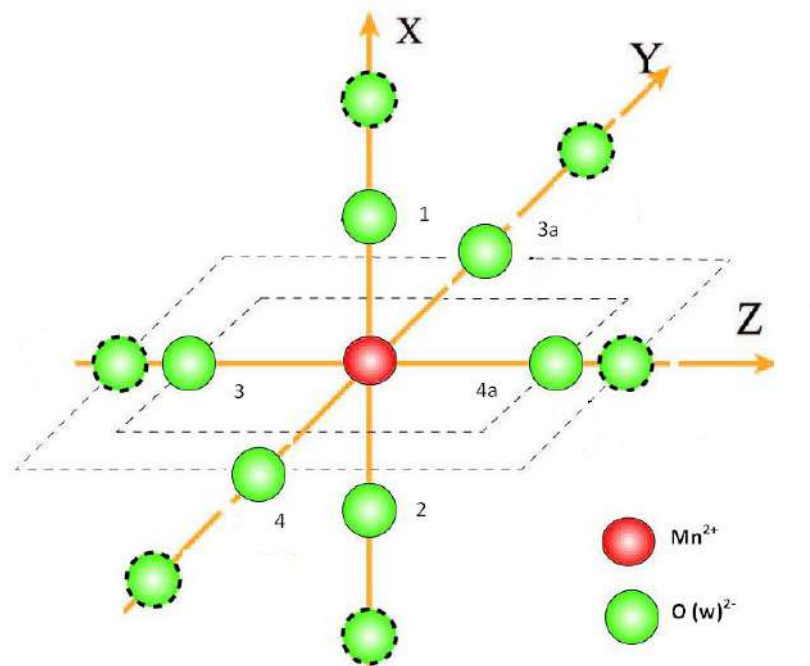
Figure and Tables

Fig 1. Crystal structure of MAP with symmetry adopted axis system (SAAS).

Table 1. Atomic coordinates in MAP crystal and bond length R (without and with distortion) along with angle θ, φ (one site).

Position of Mn^{2+}	Ligands	x	y	z	R(nm) (Å)	θ^0		φ^o	
			Without distortion						
	Mg	0	0.37648	0.37185					
Site I: Substitutional	O(W1)	0	0.68219	0.28610	0.2107	R_1	92.33	θ_1 90	φ_1
	O(W2)	0	0.08012	0.46510	0.2097	R_2	87.45	θ_2 90	φ_2
	O(W3)	0.21797	0.26377	0.26205	0.2068	R_3	93.04	θ_3 83.94	φ_3
	O(W4)	0.21055	0.48534	0.48494	0.2046	R_4	86.83	θ_4 84.08	φ_4
	O(W3a)	-0.21797	0.26377	0.26205	0.2068	R_5	93.04	θ_5 96.05	φ_5
	O(W4a)	-0.21055	0.48534	0.48494	0.2046	R_6	86.83	θ_6 95.91	φ_6
			With distortion						
	O(W1)				0.2108	$R_1+\Delta R_1$			
	O(W2)				0.2098	$R_2+\Delta R_2$			
	O(W3)				0.2078	$R_3+\Delta R_3$			
	O(W4)				0.2056	$R_4+\Delta R_4$			
	O(W3a)				0.2078	$R_5+\Delta R_5$			
	O(W4a)				0.2056	$R_6+\Delta R_6$			

Table 2. Crystal field parameters and zero field splitting parameters of Mn^{2+} doped MAP single crystal.

Site	R_0(nm)	B_{20}	B_{22}	B_{40}	B_{42}	B_{44}	$\lvert D\rvert$	$\lvert E\rvert$	$\lvert E\rvert/\lvert D\rvert$	
				Crystal- field parameters (cm^{-1})				Zero-field splitting parameters (×10^{-4}cm^{-1})		
			Without distortion							
Site I $\dfrac{\overline{A_2}}{\overline{A_4}}=10$	0.104	-4724.04	3815.115	631.426	659.1422	2863.33	336.3	108.2	0.321	
			With distortion							
Site I $\dfrac{\overline{A_2}}{\overline{A_4}}=10$	0.104	-4675.62	3775.748	622..7578	650.1423	2854.727	332.2	106.4	0.320	
							Exp. 331.7	72.2	0.217	

Table 3. Experimental and calculated (CFA package) energy band positions of Mn^{2+} doped MAP single crystal.

Transition from $^6A_{1g}(S)$	Observed wave number (cm^{-1})	Calculated wave number (cm^{-1})
$^4T_{1g}(G)$	16044	
$^4T_{2g}(G)$	20433	19821, 19823, 20508, 20529, 21067, 21096
$^4E_g(G)$	24108	23037, 23550
$^4A_{1g}(G)$	24242	23567
$^4T_{2g}(D)$	26724	26163, 26209, 26384, 26441, 27304, 27324
$^4E_g(D)$	30451	30490, 30555
$^4T_{1g}(P)$	33956	33133, 33394, 33539, 34169, 35471, 35547
$^4A_{2g}(F)$	36846	36878
$^4T_{1g}(F)$	38521	38439, 38479, 38869, 38889, 39294, 39375